

Dynamical and structural insights into the smectic phase of rod-like particles

Eric Grelet¹, M Paul Lettinga², Markus Bier³,
René van Roij³ and Paul van der Schoot⁴

¹ Centre de Recherche Paul Pascal, CNRS-Université Bordeaux 1, 115 Avenue Schweitzer, 33600 Pessac, France

² IFF, Institut Weiche Materie, Forschungszentrum Jülich, D-52425 Jülich, Germany

³ Institute for Theoretical Physics, Utrecht University, Leuvenlaan 4, 3584 CE Utrecht, The Netherlands

⁴ Department of Applied Physics, Eindhoven University of Technology, PO Box 513, 5600 MB Eindhoven, The Netherlands

E-mail: grelet@crpp-bordeaux.cnrs.fr

Received 31 July 2008, in final form 15 August 2008

Published 12 November 2008

Online at stacks.iop.org/JPhysCM/20/494213

Abstract

Self-diffusion in a model system of rod-like particles is studied in the smectic (or lamellar) phase. The experimental system is formed by a colloidal suspension of filamentous *fd* virus particles, which allows the direct visualization at the scale of the *single* particle of mass transport between the smectic layers. Self-diffusion takes place preferentially in the direction normal to the smectic layers and occurs in steps of one rod length, reminiscent of a hopping-type of transport. The probability density function is obtained experimentally at different times and is found to be in qualitative agreement with theoretical predictions based on a dynamical density functional theory.

(Some figures in this article are in colour only in the electronic version)

1. Introduction

The self-organization into liquid crystalline states is a field of intensive research, both theoretically [1] and experimentally [2, 3]. Recently, the dynamics of such self-assembled anisotropic media has been investigated in particular by the determination of self-diffusion coefficients in different kinds of mesophases [4]. These measurements have been performed with experimental techniques probing the samples *collectively* (ensemble averaged), such as in nuclear magnetic resonance (NMR) for thermotropic [5] and amphiphilic [6] liquid crystals, and fluorescence recovery after photobleaching (FRAP) for lyotropic (colloidal) systems [7]. Only a few studies have been performed where dynamical phenomena are tracked at the scale of the *single* anisotropic particle [8, 9].

In this work, the model system of aqueous dispersion of filamentous virus *fd* particles, which exhibit a highly monodisperse length and width distribution and the ability to be visualized individually by fluorescence microscopy, has been used to explore the time-dependent phenomena in the

smectic phase. In this lamellar mesophase, the particle density is quasi periodic in one dimension parallel to the long axis of the rods, while the interparticle correlations perpendicular to this axis are short-ranged (fluid-like order). In the smectic phase of *fd* virus suspensions, we investigate experimentally the process of interlayer diffusion or *permeation*, first predicted by Helfrich [10], corresponding to the jump along the long axes (or director) of *single* rod-like particles between adjacent smectic layers [9].

Here we first show that *fd* dispersions undergo a first order nematic–smectic and smectic–columnar phase transition, by using differential interference contrast microscopy. X-ray scattering is used to confirm that, within the smectic layers, rods show a Lorentzian radial distribution, typical for a liquid-like ordering, but also for a glass. Having established the structural characteristics of the smectic phase, fluorescence video microscopy is employed to study self-diffusion in this lamellar mesophase. Although particles can supposedly diffuse freely within each liquid-like layer (with diffusion coefficient D_{\perp}) but must overcome a free energy barrier to jump between adjacent layers (with diffusion coefficient D_{\parallel}), surprisingly,

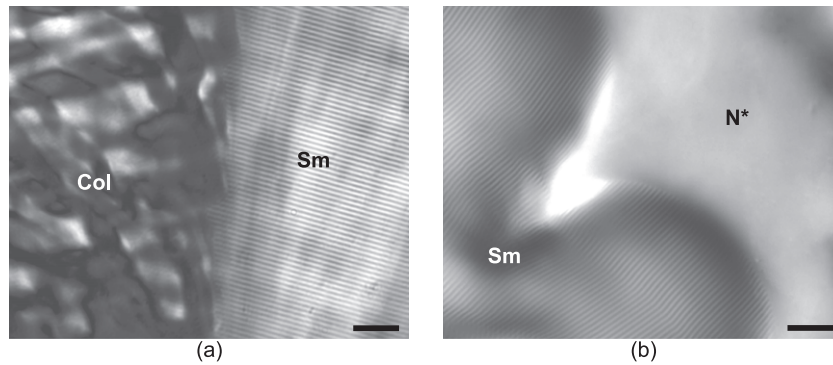


Figure 1. Phase coexistence of the different mesophases observed in aqueous suspensions of *fd* rod-like viruses by differential interference contrast microscopy. Coexistence of the (a) columnar (left) and smectic (right) phases and of the (b) smectic (left) and chiral nematic (right) phases. The scale bars indicate 10 μm in both cases.

the diffusion through the smectic layers is shown here to be much faster than the diffusion within each liquid-like layer, i.e. $D_{\parallel}/D_{\perp} \gg 1$. This behaviour will be analysed in terms of a recently developed time-dependent density functional theory [11].

2. Experimental details

2.1. Materials and methods

The system of rods used in this work consists of filamentous bacteriophages *fd*, which are semi-rigid polyelectrolytes with a contour length $L = 0.88 \mu\text{m}$, a diameter $d = 66 \text{ \AA}$, a persistence length of $2.2 \mu\text{m}$, and a molecular weight of $M_W = 1.64 \times 10^7 \text{ g mol}^{-1}$. *fd* was grown using the XL1-Blue strain of *E. Coli* as the host bacteria and purified following standard biological protocols [3]. In this study, the ionic strength has been fixed at $I = 20 \text{ mM}$ by a dialysis of *fd* suspensions against a TRIS-HCl-NaCl buffer at $\text{pH} = 8.2$. At this pH, the *fd* charge density is about $10 e \text{ nm}^{-1}$. The virus concentrations were measured using spectrophotometry with an absorption coefficient of $3.84 \text{ cm}^2 \text{ mg}^{-1}$ at 269 nm . Video fluorescence microscopy has been used to monitor the dynamics of individual labelled colloidal rods in the background of a smectic mesophase formed by identical but unlabelled rods, where about one *fd* rod out of 10^4 has been labelled with the dye Alexa-488 (Invitrogen). The colloidal scale of the *fd* bacteriophage enables the imaging of individual rods by fluorescence microscopy, as well as smectic layers by differential interference contrast (DIC) microscopy [3].

2.2. Phase diagram and structural investigations

Suspensions of *fd* rods in aqueous solution form several lyotropic liquid crystalline phases with increasing particle concentration, ranging from the chiral nematic (N^*) [12] via the smectic (Sm) [9, 13] to columnar (Col) and crystalline phases [14]. The existence of a smectic phase in suspensions of hard rods is an evidence of the high monodispersity in the particle length and therefore of the model system character of such filamentous viruses [15]. A conceptually appealing intuitive explanation for the appearance of the smectic phase

was given by Wen and Meyer [16], and it goes as follows. In the uniaxial nematic phase, neighbouring rods overlap each other by random amounts along their principal direction. This creates volumes at the end of every rod, which are accessible only to that rod but not to any other rod. In the smectic phase, with rods distributed in layers, the random overlapping of rods along their length is avoided, so these excluded volumes disappear, thereby increasing the free volume of the system. Hence, though positional entropy is lost at the transition to the smectic phase, freely available volume is gained and therefore the overall configurational entropy increases.

At $I = 20 \text{ mM}$, the typical virus concentration for the smectic phase to occur is 115 mg ml^{-1} , which corresponds to a volume fraction $\phi = 0.13$. The volume fraction has been calculated with the bare virus diameter, and not with an effective diameter taking into account the electrostatic interactions between rods. Figure 1 presents the phase coexistence of the smectic phase with the chiral nematic and columnar mesophases, respectively. Both Col-Sm and Sm- N^* phase transitions are first order, and they are fully reversible by dilution or concentration of the sample. Note that a sufficiently pronounced particle length polydispersity has been shown to rule out the smectic phase [15] and that rod flexibility also destabilizes the smectic organization [17]. Another consequence of the virus flexibility is that the smectic layer spacing is very close to the particle length [18, 13].

In order to study the nature of the positional order within the smectic layers, small angle x-ray scattering (SAXS) has been performed at the ESRF-ID02 beamline (Grenoble, France). Figure 2(a) presents the average radial intensity in the wavevector range suitable for probing the interaxial organization of the rods. The position of the Bragg peak is $q_{100} = 0.0492 \text{ \AA}^{-1}$, which corresponds to a distance between rods of $d_{\text{inter}} = 4\pi/\sqrt{3}q_{100} = 147 \text{ \AA}$. In a conventional liquid the positional correlations decay exponentially with distance, giving a Lorentzian scattering profile of the Bragg reflections. A line shape analysis of the first order Bragg peak has been performed as shown in figure 2(b): a Lorentzian distribution almost perfectly fits the data. A positional correlation length of $\xi = 2\pi/\text{FWHM} = 540 \text{ \AA}$ is found, which corresponds to an inter particle correlation extending up to about four neighbours.

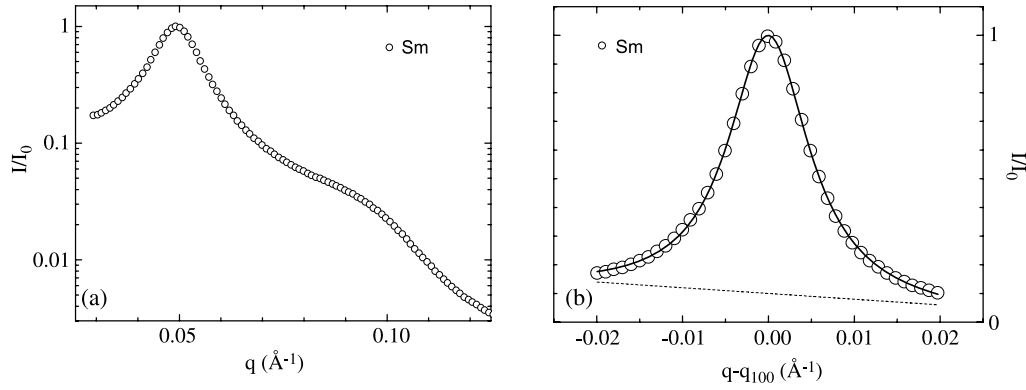


Figure 2. (a) Average radial intensity as a function of the scattering wavevector, probing the inter-rod structure within the smectic layer. (b) Lorentzian fit (solid line) of the first order Bragg reflection (open symbols) which are not resolution limited. The dashed line shows the subtracted linear background.

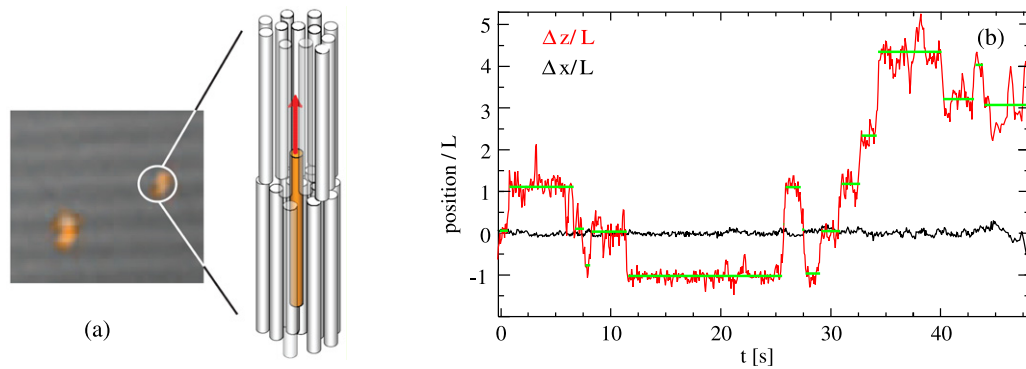


Figure 3. (a) Overlay of differential interference contrast and fluorescence images, showing the smectic layers and two fluorescently labelled particles, and the schematic representation of the jump of rod-like particles between adjacent smectic layers. The layer spacing is $L \simeq 0.9 \mu\text{m}$. (b) Displacement of a given particle in the direction parallel (red line) and perpendicular (black line) to the normal of the smectic layers. The horizontal green lines indicate the residence time, i.e. the time for which one particle stays in a given layer.

This demonstrates that the structure of the order is liquid-like in the layers of the smectic phase.

2.3. Self-diffusion of single particles

Figure 3(a) shows an example of images of a single region where both DIC and fluorescence techniques are combined: some rods jump between two layers while others remain within a given layer. The trajectory of one of the rods is plotted in figure 3(b) in the direction parallel (z) and perpendicular (x) to the director. The main result of our measurements is the following: diffusion between the smectic layers takes place in *quasi-quantized steps* of one rod length, and the diffusion within the smectic layer is extremely slow.

The ‘hopping-type’ diffusion is the consequence of the underlying ordering potential of the smectic phase and the vacancies available in adjacent layers. It shows that the mass transport between the layers is a discontinuous process, as evidenced by the self-Van Hove function $G(z, t)$ in figure 4(a) [19], which is defined as the probability density for a displacement z during a time interval t :

$$G(z, t) = \frac{1}{N} \left\langle \sum_{i=1}^N \delta[z + z_i(0) - z_i(t)] \right\rangle. \quad (1)$$

For an uniform fluid of Brownian particles, a smooth Gaussian distribution that smears out over time is expected for the self-Van Hove function. In the smectic phase, however, $G(z, t)$ shows distinct peaks exactly at integer multiples of the particle length (and therefore of the layer thickness), as also inferred from visual inspection of the rod trajectories (figure 3).

2.4. Mean square displacement

The overall mean square displacement (MSD) of rods parallel and perpendicular to the director of the smectic and nematic phases is plotted in figure 4(b). Here parallel MSD is scaled by the length of the rod L , while the time is scaled by the time it takes to diffuse one rod length in the nematic phase, i.e. $\tau_L = L^2/D_{\parallel}^{\text{nem}}$. Similarly, the perpendicular MSD is scaled by the rod diameter d , while the time is scaled by the time it takes to diffuse one rod thickness in the nematic phase, i.e. $\tau_d = d^2/D_{\perp}^{\text{nem}}$. The time evolution of the MSD given by $\langle \Delta r^2(t) \rangle \sim t^\gamma$ provides the diffusion exponent γ : $\gamma < 1$ is characteristic of a *sub* diffusive behaviour, while $\gamma > 1$ is referred to as *super* diffusion. The parallel motion is close to be diffusive in the (chiral) nematic phase ($\gamma = 0.95$) close to the N*-Sm phase transition over the whole studied time range, i.e. over several rod lengths. However, the parallel motion in

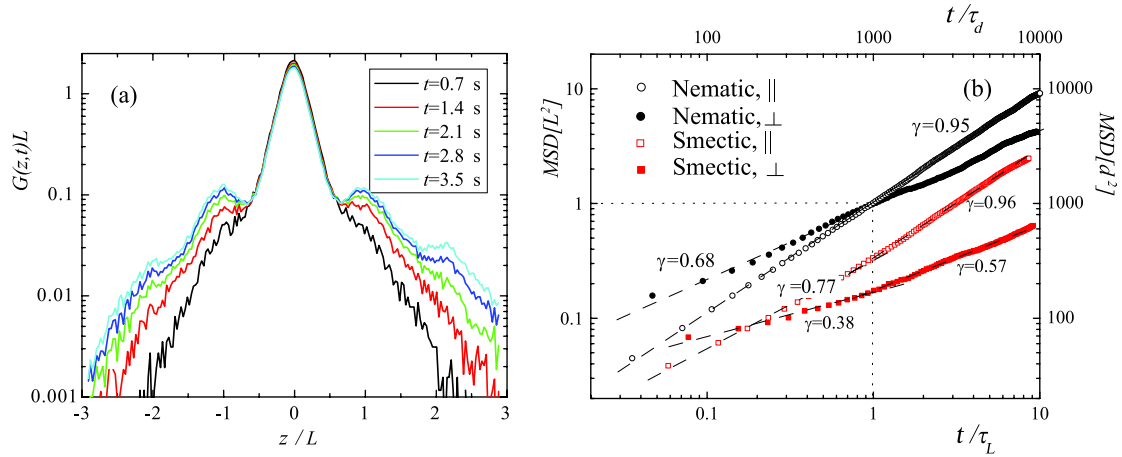


Figure 4. (a) Evolution of the self-Van Hove function at different times. The functions are normalized to one, the z -axis is scaled by the smectic layer thickness L . (b) Log-log representation of the scaled mean square displacement (MSD) parallel and perpendicular to the director in the nematic and smectic phases (see legend) versus the scaled time. The dotted lines indicate the time the rods diffuse one rod length. The dashed lines represent the numerical fits by a power law.

the smectic phase is significantly sub diffusive for $t < \tau_L$: $\gamma = 0.77$, while it is diffusive for $t > \tau_L$ ($\gamma = 0.96$). The perpendicular motion is, in both cases, strongly sub diffusive. In the nematic phase $\gamma = 0.68$, while in the smectic phase once again two regimes can be distinguished: $\gamma = 0.38$ for $t < 1000\tau_d$ and $\gamma = 0.57$ for $t > 1000\tau_d$.

3. Theoretical details

In order to theoretically study the diffusion in uniform and non-uniform complex fluids, a general method was put forward allowing for the straightforward calculation of Van Hove correlation functions within dynamical density functional theory [11]. Because the *fd* virus filaments can be considered as long, thin rods of high stiffness (see section 2.1) that are strongly aligned in the nematic and smectic phases, one can in a first approximation neglect the orientational degrees of freedom [20] and model a liquid crystalline *fd* virus dispersion as a fluid of aligned hard rods of an effective length and diameter. Within the dynamical density functional theory we next invoke the second virial approximation [21], which is not quite exact at the densities where the smectic phase is stable but contains the relevant physics, and numerically solve the relevant kinetic equations that link the self-diffusion of a test particle to the collective diffusion of all the other particles in the system.

In figure 5 we compare the self-Van Hove correlation function $G(z, t)$ obtained from our model calculations with the measurements displayed in figure 4. Here L denotes the smectic layer spacing and τ_L is the parallel diffusion time $\tau_L = L^2/D_{\parallel}^{\text{short}}$, where $D_{\parallel}^{\text{short}}$ is the short-time parallel diffusion. The model parameters for the smectic state in the calculation were chosen such that the smectic ordering potential barriers correspond to those determined in the experiment from a Boltzmann weighting of the density profiles [9].

Figure 5 shows that even a calculation at the level of the second virial approximation can account for the

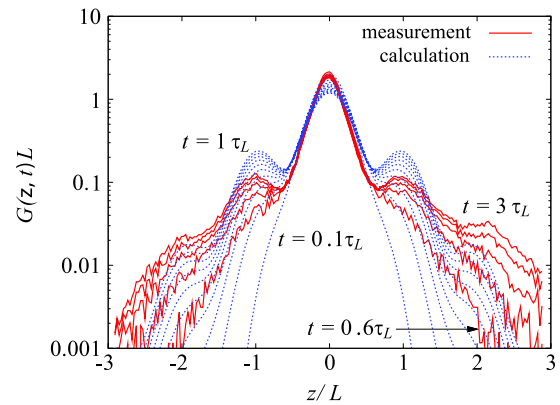


Figure 5. The self-Van Hove correlation function $G(z, t)$ obtained within the dynamical density functional calculation based on a highly idealized second virial model of perfectly aligned, perfectly rigid hard rods, indicated by the blue dotted lines, exhibits the qualitative features of the measurement (red solid lines). Here L is the smectic layer spacing and τ_L is a parallel diffusion time. The quantitative differences can be attributed to an overestimation of the compressibility and the neglect of the particle bending flexibility within the theoretical model.

qualitative features of the non-trivial, hopping-type diffusive behaviour of rod-like particles along the director from one smectic layer to the next. The quantitative differences between the measurements and theory can be understood by realizing that the second virial approximation overestimates the compressibility of the fluid. Indeed, a rod in the model fluid can, compared to a real *fd* virus, more easily squeeze into a neighbouring layer, which increases the decay rate in the central region around $z = 0$ and the growth rate of the first side peaks around $z = \pm L$ in figure 5. The height of the peaks around $z = \pm 2L$ is associated with the cooperative movement of a rod from the central layer via a void in the first layer to the second layer, which is more pronounced in the experiment than in the calculation.

4. Discussion

Anomalous sub diffusive behaviour has often been observed in systems where diffusion involves an initial waiting time, e.g. following the release of a test particle from a temporary cage caused by the presence of other particles [22]. It stands to reason that this ‘cage escape’ might be at the root of the observed sub diffusive behaviour for both parallel and perpendicular diffusion observed in the smectic phase. For parallel diffusion of rods the cage is actually formed by the free energy barrier imposed by the smectic layers, superimposed on which is the effective barrier from the enhanced number of particles that cage the central (test) particle [11]. Indeed in both the experiments and the calculations (see also figure 3(a) of [11]) the parallel behaviour is sub diffusive for $t < \tau_L$, related to the crossover between short-time and long-time diffusive behaviour.

The anisotropy in the diffusivities, D_{\parallel}/D_{\perp} , which is about 20 in the nematic phase [8], increases in the smectic phase within the measured time range as a result of the pronounced sub diffusivity of the perpendicular motion (as indicated by the decrease of γ). Since this sub diffusive behaviour lasts for the whole studied time range, i.e. thousands of rod diameters, it seems that the rods in the layers are glass-like rather than liquid-like. This observation is apparently opposite to the trend found for thermotropic liquid crystals, where usually D_{\parallel}/D_{\perp} decreases due to an Arrhenius form of the diffusion constants [4, 5]. Also note that preliminary results by Dogic on the self-diffusion of *fd* virus particles in single lamellar membranes indicate that without neighbouring layers perpendicular diffusion is much faster [23].

The cause of the experimentally observed perpendicular sub diffusive behaviour is not clear *a priori*. The theoretical calculations show diffusive long-time behaviour in the perpendicular direction; it should be realized, however, that both flexibility and orientational degrees of freedom are not taken into account in the theory, both of which will result in significant excluded volume effects. Thus, the dominant mode of perpendicular diffusion could be a repetition-like parallel motion of the rod along the long axis to escape its locally excluded volume, similar in nature to what is observed for polymers in the dense melt, for which typically $\gamma = 0.5$ [24]. Including these effects could also help to explain the discrepancy between the envelope of the measured and calculated Van Hove functions plotted in figure 5, since the experimentally observed $\sim z^{-1}$ behaviour could be related to the relaxation of voids once a rod has jumped between two adjacent layers.

5. Summary

We have shown by means of real-space video fluorescence microscopy that the diffusive transport of particles between the layers of a smectic lyotropic colloidal liquid crystal is a discontinuous process that occurs in steps of one layer spacing. Our approach using the dynamical density functional theory, which is found to describe qualitatively the underlying dynamics, points out the importance of the existence of free

energy barriers between the smectic layers. This gives rise to a kinetics where particles hop from one layer to the other with a time scale which is dictated by the height of the barriers. At shorter time scales, the particles remain trapped in the smectic layers and perform a diffusive ‘bobbing’ motion about the local minimum of the self-consistent molecular field.

Acknowledgments

We thank Marjolein Dijkstra for suggesting the application of DDFT to smectics of rods. This project was supported by the European Network of Excellence SoftComp and Transregio Sonderforschungsbereich TR6018 ‘Physics of Colloidal Dispersions in External Fields’. This work is part of the research programme of the ‘Stichting voor Fundamenteel Onderzoek der Materie (FOM)’, which is financially supported by the ‘Nederlandse Organisatie voor Wetenschappelijk Onderzoek (NWO)’.

References

- [1] Frenkel D, Lekkerkerker H N W and Stroobants A 1988 *Nature* **332** 822
Vroege G J and Lekkerkerker H N W 1992 *Rep. Prog. Phys.* **55** 1241
- [2] Wen X, Meyer R B and Caspar D L D 1989 *Phys. Rev. Lett.* **63** 2760
Davidson P and Gabriel J C P 2005 *Curr. Opin. Colloid Interface Sci.* **9** 377
Dogic Z and Fraden S 2006 *Curr. Opin. Colloid Interface Sci.* **11** 47
- [3] Dogic Z and Fraden S 2006 *Soft Matter* vol 2, ed G Gompper and M Schick (Weinheim: Wiley-VCH)
- [4] Hess S, Frenkel D and Allen M P 1991 *Mol. Phys.* **74** 765
Löwen H 1999 *Phys. Rev. E* **59** 1989
Selinger R L B 2002 *Phys. Rev. E* **65** 051702
Bates M A and Luckhurst G R 2004 *J. Chem. Phys.* **120** 394
Cifelli M, Cinacchi G and De Gaetani L 2006 *J. Chem. Phys.* **125** 164912
- [5] Krüger G J 1982 *Phys. Rep.* **82** 229
Dvinskikh S V, Furo I, Zimmermann H and Maliniak A 2002 *Phys. Rev. E* **65** 061701
- [6] Blinc R, Easwaran K, Pirs J, Volfan M and Zupancic I 1970 *Phys. Rev. Lett.* **25** 1327
Gaemers S and Bax A 2001 *J. Am. Chem. Soc.* **123** 12343
Hubbard P L, McGrath K M and Callaghan P T 2005 *Langmuir* **21** 4340
- [7] Bu Z, Russo P S, Tripton D L and Negulescu I I 1994 *Macromolecules* **27** 6871
van Bruggen M P B, Lekkerkerker H N W, Maret G and Dhont J K G 1998 *Phys. Rev. E* **58** 7668
Cush R C and Russo P S 2002 *Macromolecules* **35** 8659
- [8] Lettinga M P, Barry E and Dogic Z 2005 *Europhys. Lett.* **71** 692
- [9] Lettinga M P and Grelet E 2007 *Phys. Rev. Lett.* **99** 197802
- [10] Helfrich W 1969 *Phys. Rev. Lett.* **23** 372
- [11] Bier M, van Roij R, Dijkstra M and van der Schoot P 2008 arXiv:0807.4089
- [12] Lapointe J and Marvin D A 1973 *Mol. Cryst. Liq. Cryst.* **19** 269
Dogic Z and Fraden S 2000 *Langmuir* **16** 7820
Grelet E and Fraden S 2003 *Phys. Rev. Lett.* **90** 198302
Tombolato F, Ferrarini A and Grelet E 2006 *Phys. Rev. Lett.* **96** 258302
- [13] Dogic Z and Fraden S 1997 *Phys. Rev. Lett.* **78** 2417

- [14] Grelet E 2008 *Phys. Rev. Lett.* **100** 168301
- [15] Bates M A and Frenkel D 1998 *J. Chem. Phys.* **109** 6193
- [16] Wen X and Meyer R B 1987 *Phys. Rev. Lett.* **59** 1325
- [17] Hentschke R and Herzfeld J 1991 *Phys. Rev. A* **44** 1148
Selinger J V and Bruinsma R F 1991 *Phys. Rev. A* **43** 2922
van der Schoot P 1996 *J. Physique II* **6** 1557
- [18] van der Schoot P 1997 *J. Physique II* **6** 1557
Tkachenko A V 1996 *Phys. Rev. Lett.* **77** 4218
- [19] Hansen J P and McDonald I R 1986 *Theory of Simple Liquids* (London: Academic)
- [20] Odijk T 1986 *Macromolecules* **19** 2313
- [21] Mulder B 1987 *Phys. Rev. A* **35** 3095
- [22] Weeks E R and Weitz D A 2002 *Phys. Rev. Lett.* **89** 095704
- [23] Dogic Z 2008 private communication
- [24] McLeish T C B 2002 *Adv. Phys.* **51** 1379